



Contents lists available at ScienceDirect

The Saudi Dental Journal

journal homepage: www.ksu.edu.sa
www.sciencedirect.com

Original Article

Evaluation of the shaping ability of different rotary file systems in severely and abruptly curved root canals using cone beam computed tomography

Chanapa Damkoengsunthon^a, Adjabhak Wongviriya^b, Weeraya Tantanapornkul^b,
Kessiri Wisithphrom^a, Kittipong Ketpan^a, Thosapol Piyapattamin^c,
Peraya Puapichartdumrong^{a,*}^a Department of Restorative Dentistry, Faculty of Dentistry, Naresuan University, Thailand^b Department of Oral Diagnosis, Faculty of Dentistry, Naresuan University, Thailand^c Department of Preventive Dentistry, Faculty of Dentistry, Naresuan University, Thailand

ARTICLE INFO

Keywords:

Canal centering
Danger zone
Remaining dentin thickness
Root canal preparation
Rotary file
Transportation

ABSTRACT

Background: When selecting an instrument for canal preparation, it is important to consider several parameters that influence the shaping efficiency, including instrument design, metallurgy, and operating motion. This study aimed to evaluate the shaping ability of the ProTaper Next (PTN), WaveOne Gold (WOG), and XP-endo Rise Shaper (XPRS) rotary systems in severely and abruptly curved root canals using cone beam computed tomography (CBCT) and ImageJ software.

Materials and Methods: Forty-eight mesial root canals of the mandibular first molars were assigned equally to three groups: PTN, WOG, and XPRS. Using ImageJ software, CBCT images were acquired pre- and post-instrumentation to assess dentin removal, remaining dentin thickness (RDT), canal transportation, and centering ratio at the coronal, middle, and apical levels. Statistical analyses were conducted on all numerical data.

Results: All rotary systems removed significantly more distocoronal dentin in the danger zone (DZ), than the mesiocoronal area. PTN removed significantly more dentin and caused less RDT than XPRS ($p < 0.05$). However, there were no significant differences between PTN-WOG and WOG-XPRS. In the DZ, the highest percentage of specimens with an RDT < 0.5 mm was observed when using PTN (50%), followed by WOG (31.3%), and XPRS (6.3%). Compared with PTN and WOG, XPRS demonstrated less coronal transportation. Among all rotary systems, there was no significant difference in apical transportation or centering ratio.

Conclusions: Based on our observations, all rotary instruments exhibited a tendency to remove dentin in the DZ, but to different degrees. XPRS demonstrated better results in terms of coronal transportation and dentin thickness in the DZ. Comparable centering abilities and minimal apical transportation were demonstrated using all rotary instruments.

1. Introduction

Preserving the original canals and root structure is crucial for successful root canal preparation (Peters and Peters, 2011). The thin distal wall of the mesial root is caused by the furcal concavity of the mandibular first molar, particularly in the coronal third area (Nanbunta et al., 2024), which is also known as the danger zone (DZ) (Abou-Rass et al., 1980). Overinstrumentation can cause strip perforations, leading to treatment failure. Although the optimal remaining dentin thickness

(RDT) is not well defined, Lim and Stock (1987) suggest that lateral condensation requires > 0.30 mm of dentin to prevent perforation. The risk of perforation increases if dentin thickness, 3–4 mm below the furcation, is < 0.50 mm (Zhou et al., 2020). Instrumentation is more challenging in severely and abruptly curved root canals. The restraining force of the instrument can cause apical transportation and canal straightening (Bürklein and Schäfer, 2013).

Innovative nickel-titanium (NiTi) instruments have been developed to enhance the efficacy of root canal treatment. The use of more flexible

* Corresponding author at: Department of Restorative Dentistry, Faculty of Dentistry, Naresuan University, Phitsanulok 65000, Thailand.

E-mail addresses: chanapad64@nu.ac.th (C. Damkoengsunthon), adjabhakw@nu.ac.th (A. Wongviriya), weerayat@nu.ac.th (W. Tantanapornkul), kessiriw@nu.ac.th (K. Wisithphrom), kittitongk@nu.ac.th (K. Ketpan), thosapolp@nu.ac.th (T. Piyapattamin), perayap@nu.ac.th (P. Puapichartdumrong).

<https://doi.org/10.1016/j.sdentj.2024.07.016>

Received 10 May 2024; Received in revised form 28 July 2024; Accepted 31 July 2024

Available online 2 August 2024

1013-9052/© 2024 THE AUTHORS. Published by Elsevier B.V. on behalf of King Saud University. This is an open access article under the CC BY-NC-ND license (<http://creativecommons.org/licenses/by-nc-nd/4.0/>).

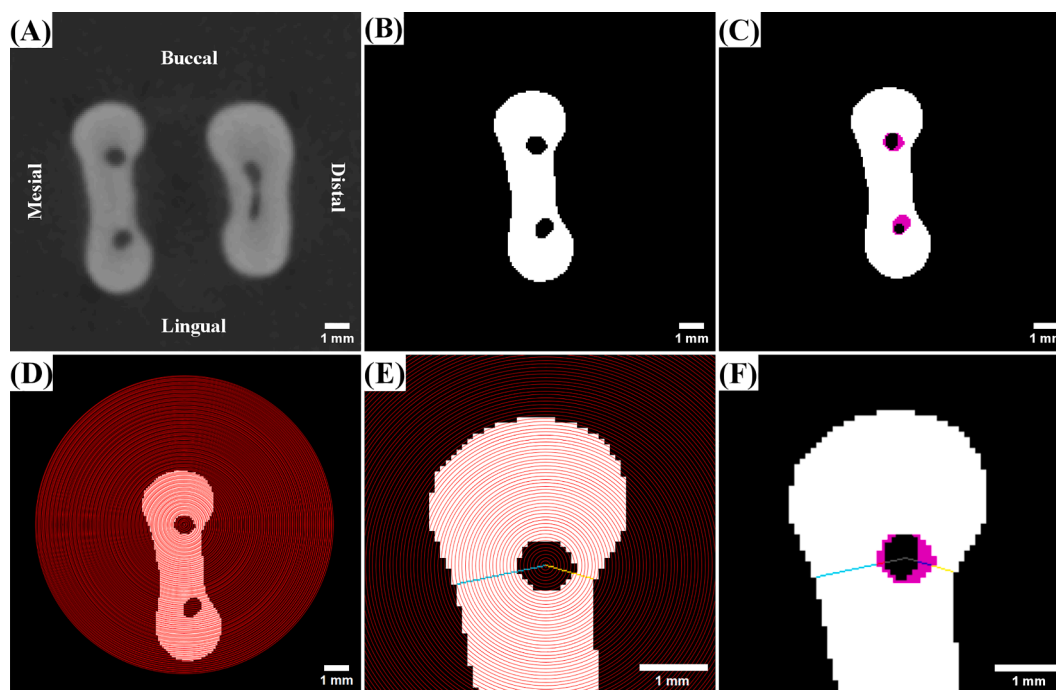


Fig. 1. A cross-sectional cone beam computed tomographic image of the mesial root of a human mandibular first molar (A), a segmented mesial root image (B), perfectly superimposed pre- and post-instrumentation images (C), superimposed images with one hundred concentric circles created from the canal centroid in the aligned post-instrumentation image (D), the shortest radius at the mesial (cyan line) and distal (yellow line) sides (E), representative images of minimum dentin thickness pre-instrumentation (M1; red and cyan lines, and D1; blue and yellow lines), and post-instrumentation (M2; cyan line, and D2; yellow line (F).

NiTi rotary files instead of stainless-steel hand files can reduce canal transportation and errors (Zupanc et al., 2018). ProTaper Next (PTN; Dentsply Sirona, Ballaigues, Switzerland) is a rotary file made of an M-Wire with an off-center rectangular cross-section and a variable taper (Ruddle et al., 2013). It demonstrated higher cyclic fatigue resistance than ProTaper Universal, which is made of a conventional NiTi alloy (Dentsply Sirona) (Uygun et al., 2016). The PTN is recommended for continuous rotation motion with brushing movement and is suitable for anticurvature filing to prevent overinstrumentation in the DZ (Lim and Stock, 1987; Sousa et al., 2022).

WaveOne Gold (WOG; Dentsply Maillefer, Ballaigues, Switzerland) is a reciprocating single-file system featuring two cutting edges, an offset parallelogram cross-section, and a regressive taper. Gold alloy increases WOG's flexibility compared to the previous M-Wire version (Ruddle, 2016).

The new XP-endo Rise Shaper (XPRS; FKG Dentaire, La Chaux-de-Fonds, Switzerland) features a triangular cross section and a unique 6-cutting-edge booster tip, differentiating it from the XP-endo Shaper (XPS) version. Made from Max-Wire alloy, it can expand from a size of 30/0.01 to at least 30/0.04 at temperatures $\geq 35^\circ\text{C}$. XPS has shown high resistance to cyclic fatigue (Silva et al., 2018) and can adapt well to the root canal anatomy during instrumentation (Azim et al., 2017).

When selecting an instrument for canal preparation, it is important to consider several parameters that influence the shaping efficiency, including the instrument's design, metallurgy, and operating motion (Liang and Yue, 2022). The shaping performances of the PTN, WOG, and XPS have been documented in the literature (de Albuquerque et al., 2019; Shaheen and Elhelbawy, 2022); however, comparisons of severely and abruptly curved root canals are not available.

Cone beam computed tomography (CBCT) is valuable for evaluating root canal structure, including dentin thickness (Bunn et al., 2020; Mangal et al., 2018). It provides high-resolution three-dimensional (3D) information and is nondestructive to samples. ImageJ software, developed by the National Institutes of Health, is often used to analyze CBCT images. Because of its accuracy and reproducibility, this method has

been used to assess periodontal osseous defects (Aditya and Vandana, 2023) and dentin thickness (Yang et al., 2015). Hence, this study aimed to evaluate the shaping ability of the PTN, WOG, and XPRS rotary systems in severely and abruptly curved root canals using CBCT and ImageJ software.

2. Materials and Methods

2.1. Sample selection

This study was approved by Naresuan University Human Research Ethics Committee (IRB No. P1-0019/2566). Forty-eight mesial root canals from extracted human mandibular first molars were collected from dental clinic waste. Buccolingual and mesiodistal periapical radiographs were obtained using a digital X-ray device (Myray; Cefla Dental Group, Imola, Italy; 65 kVp, 6 mA, 1 s exposure). The canal configurations and preliminary measurements of the angle (Schneider, 1971) and radius (Pruett et al., 1997) of the root canal curvature were evaluated. Inclusion criteria were complete root formation, type IV canal configuration (Vertucci, 1984), a 25° – 43° curvature angle, and a radius > 4 mm and ≤ 8 mm. The exclusion criteria included dental anomalies, prior root canal treatments, restorations below the cemento-enamel junction, root caries, internal or external root resorption, or calcified canals that could not be negotiated with a #10 K-file (Dentsply Sirona). The remaining tissue and calculus were removed, and the teeth were stored in 10% formalin until use.

2.2. Sample preparation and CBCT imaging

A high-speed diamond bur (#2; Jota AG, Rüthi, Switzerland) was used to create access openings in each tooth. Subsequently, the tooth was mounted in a clear acrylic resin (Orthocryl; Dentaaurum, Ispringen, Germany) block and positioned in an acrylic mold on the chin rest of the CBCT scanner to ensure consistent positioning. Samples were scanned using CBCT (3D Accutomo XYZ Slice View Tomograph, Kyoto, Japan; 90

kVp, 5 mA, 0.08 mm voxel size, and 40 × 40 mm field of view). The exact angle and radius of the root canal curvature of the mesiobuccal (MB) and mesiolingual (ML) canals were remeasured using CBCT images and ImageJ software (version 1.54 h). The root canals were purposefully divided into three rotary groups, ensuring an equal number of canals with similar curvature angles and radii.

The root canal, containing a #10 K-file, was subjected to periapical radiography with a 20° mesial tube shift. The root length was measured (average 10.0 ± 2.0 mm), and the working length was calculated by deducting 1 mm. A glide path was prepared using a #15 K-file with RC-Prep (Well-Prep, Vericom Co., Anyang, Korea) as a lubricant. The root canals were irrigated with 2.5% NaOCl (10 ml total) at room temperature using a 27-gauge needle, delivering 2 ml of irrigant every 2–3 mm of file penetration. After the final rinse, the root canals were recapitulated using a #10 K-file and dried using paper points. One instrument was used for each of the five root canals. The preparation was complete when the final instrument reached its full working length.

All rotary systems were used with X-smart Plus endodontic motors (Dentsply Sirona) at the recommended speed and torque settings. In the PTN group, the root canals were instrumented with a brushing motion toward the mesial side using an Xa orifice opener with a tip diameter and taper of 19/0.035, followed by X1 (17/0.04), X2 (25/0.06), and X3 (30/0.07) files.

In the WOG group, coronal preflaring was performed using the WOG primary file (25/0.07), followed by the primary and medium (35/0.06) files until the working length was reached using an in-and-out motion.

In the XPRS group, samples were immersed in a 40 °C water bath during instrumentation to maintain a temperature ≥ 35 °C inside the root canals. Canals were instrumented using the XPRS (30/0.01) with in-and-out motion and gentle 2–3 mm strokes until the working length was achieved.

2.3. Image analysis

CBCT scanning using ImageJ was used to quantify dentin removal, RDT, canal transportation, and the centering ratio. The region between the furcation and the root apex of the mesial roots was subdivided into three equidistant levels: coronal, middle, and apical. Each root was cross-sectionally sliced, 0.08 mm thick, perpendicular to its long axis. Representative images at each level were selected from cross-sectional images in the median vertical plane.

The minimum dentin thickness (MDT) of the mesial root canals was determined using ImageJ. Pre- and post-instrumentation images were prepared (Figs. 1A and 1B) and merged in different color channels for perfect superimposition (Fig. 1C) using aligned RGB planes (Landini, 2004). MDTs were identified from the aligned post-instrumentation images with canal centroids located using the Find Maxima command. Concentric circles were generated around each root canal centroid (Fig. 1D), and a reference line was drawn from the centroid to the intersection of the innermost concentric circle with the external root surface (Fig. 1E) to measure the MDTs, labeled M1, D1, M2, and D2 (Fig. 1F).

Table 1
Mean ± standard deviation of dentin removal (mm) at three root canal levels.

Level	Dentin removal (mm)					
	Mesial			Distal		
	PTN	WOG	XPRS	PTN	WOG	XPRS
Coronal	0.166 ± 0.082 ^{A,*}	0.141 ± 0.078 ^{A,*,#}	0.093 ± 0.049 ^{A,#}	0.458 ± 0.127 ^{B,*}	0.372 ± 0.104 ^{B,*,#}	0.211 ± 0.094 ^{B,#}
Middle	0.260 ± 0.169 ^{A,*}	0.166 ± 0.076 ^{A,*,#}	0.096 ± 0.052 ^{A,#}	0.235 ± 0.157 ^{A,*}	0.154 ± 0.092 ^{A,*}	0.161 ± 0.057 ^{B,*}
Apical	0.158 ± 0.071 ^{A,*}	0.108 ± 0.051 ^{A,*}	0.130 ± 0.060 ^{A,*}	0.105 ± 0.060 ^{B,*}	0.119 ± 0.058 ^{A,*}	0.099 ± 0.049 ^{A,*}

Different superscript majuscules and symbols indicate significant differences between sides and rotary systems within the same row, according to an independent *t*-test and a one-way analysis of variance (*p* < 0.05).

Abbreviations: PTN, ProTaper Next; WOG, WaveOne Gold; XPRS, XP-endo Rise Shaper.

The amount of dentin removal was calculated using formulas for the mesial (M1 – M2) and distal (D1 – D2) sides. The minimum thickness after instrumentation was reported as RDT (M2 and D2). An RDT of < 0.5 mm at each level was calculated.

The (M1 – M2) – (D1 – D2) equation was used to quantify canal transportation. A value of 0 indicated the absence of transportation, with negative and positive values indicating deviations toward the distal and mesial sides, respectively.

The equation (M1 – M2)/(D1 – D2) or (D1 – D2)/(M1 – M2) was used to determine the centering ratio. A result of 1 indicates the file remained in the center of the root canal, whereas a value close to 0 suggests a decreased capacity to retain the file in the center of the root canal (Gambill et al., 1996).

2.4. Statistical analysis

SPSS (version 23.0; IBM, Armonk, New York, USA) was used to analyze numerical data. The Shapiro-Wilk test was used to assess the normal distribution of the data. Dentin removal and RDT values under the assumption of normalcy were analyzed among rotary systems using a one-way analysis of variance and *post-hoc* Tukey HSD test, and between sides using an independent *t*-test. Canal transportation and centering ratio data with abnormality assumptions were analyzed among the levels and rotary systems using the Kruskal-Wallis and Mann-Whitney U tests. Statistical significance was set at *p* < 0.05.

3. Results

Dentin removal and RDT differed significantly among the three rotary systems, with *p*-values of 0.011 and 0.030, respectively (Tables 1 and 2). All file systems removed more distocoronal dentin than mesio-coronal dentin (*p* < 0.05). PTN removed more dentin and resulted in a lower RDT than XPRS (*p* < 0.05); however, no significant differences were found between PTN and WOG and between WOG and XPRS. No significant RDT differences were observed at the middle and apical levels between sides or rotary groups, except for the middle level of XPRS (*p* < 0.05). Table 3 lists the number of specimens with an RDT < 0.5 mm. Fig. 2 shows the superimposed cross-sectional pre- and post-instrumentation images for each rotary group.

Significant differences in median canal transportation were found between the levels and rotary systems (*p* = 0.000). All the rotary groups showed greater canal transportation at the coronal level, mostly toward the distal side. Compared with PTN and WOG, XPRS exhibited less coronal transportation (*p* < 0.05). At the middle level, only the WOG group’s transportation was toward the mesial side, which was significantly different from that of the XPRS group (*p* < 0.05). No significant differences in canal transportation were detected among the rotary systems at the apical level (*p* > 0.05) (Table 4).

Significant differences in median centering ratios were found among the levels (*p* < 0.05) but not among the rotary systems. PTN and WOG showed significantly better centering at the middle and apical levels than at the coronal level (*p* < 0.05) (Table 4).

Table 2
Mean \pm standard deviation of remaining dentin thickness (mm) at three root canal levels.

Level	Remaining dentin thickness (mm)					
	Mesial			Distal		
	PTN	WOG	XPRS	PTN	WOG	XPRS
Coronal	1.115 \pm 0.165 ^{A,*}	1.225 \pm 0.176 ^{A,*,#}	1.272 \pm 0.153 ^{A,#}	0.517 \pm 0.181 ^{B,*}	0.670 \pm 0.212 ^{B,*,#}	0.795 \pm 0.230 ^{B,*}
Middle	0.772 \pm 0.131 ^{A,*}	0.876 \pm 0.254 ^{A,*}	1.084 \pm 0.213 ^{A,#}	0.722 \pm 0.158 ^{A,*}	0.840 \pm 0.192 ^{A,*}	0.837 \pm 0.188 ^{B,*}
Apical	0.609 \pm 0.198 ^{A,*}	0.718 \pm 0.267 ^{A,*}	0.780 \pm 0.203 ^{A,*}	0.570 \pm 0.180 ^{A,*}	0.611 \pm 0.168 ^{A,*}	0.711 \pm 0.230 ^{A,*}

Different superscript majuscules and symbols indicate significant differences between sides and rotary systems within the same row, according to an independent *t*-test and a one-way analysis of variance ($p < 0.05$).

Abbreviations: PTN, ProTaper Next; WOG, WaveOne Gold; XPRS, XP-endo Rise Shaper.

Table 3
Number (percentage) of specimens with a remaining dentin thickness less than 0.5 mm.

Level	Number of specimens (percentage)					
	Mesial			Distal		
	PTN	WOG	XPRS	PTN	WOG	XPRS
Coronal	0	0	0	8 (50.0%)	5 (31.3%)	1 (6.3%)
Middle	0	0	0	2 (12.5%)	0	1 (6.3%)
Apical	2 (12.5%)	3 (18.8%)	0	5 (31.3%)	5 (31.3%)	3 (18.8%)

Abbreviations: PTN, ProTaper Next; WOG, WaveOne Gold; XPRS, XP-endo Rise Shaper.

4. Discussion

An inverse relationship between dentin removal and RDT was observed, with dentin removal resulting in a decreased RDT. In the DZ of mandibular molars, the safety of utilizing a large size of PTN X4 (40/0.06) and WOG medium with an RDT thicker than 0.715 mm at 3 mm below the furcation has been demonstrated (Sousa et al., 2022). However, this study found that the average distocoronal RDT in the PTN group was 0.517 mm, despite the use of a smaller X3. Additionally, this group had the highest proportion of specimens with RDT $<$ 0.5 mm. This could be due to the larger diameter and higher taper of PTN X3 compared to WOG medium and XPRS (de Albuquerque et al., 2019).

Regardless of the rotary system, brushing or the in-and-out motion removed more dentin from the distocoronal area than from the mesio-coronal area. Although the PTN was employed with a brushing motion to conserve the DZ preparation, it could not prevent dentin removal from this area. These findings corroborate those of a previous study (Bergmans et al., 2003), in which more dentin was removed toward the furcation despite efforts to brush away from the DZ for anticurvature filling.

The restraining force of the NiTi file causes coronal canal transportation toward the distal side and apical transportation toward the mesial side, as previously mentioned (Bürklein and Schäfer, 2013). XPRS exhibited significantly lower coronal transportation than WOG and PTN. This is in agreement with a previous study showing that XPRS has less coronal transportation than WOG (Shaheen and Elhelbawy, 2022) and less total transportation than PTN and WOG (Bayram et al., 2022). This might be because XPRS has a less tapered shape and is an innovative Max-Wire alloy that is flexible, resistant to cyclic fatigue, and adaptable to root canal anatomy (Azim et al., 2017; Shaheen and Elhelbawy, 2022; Silva et al., 2018). However, comparable coronal transportation was observed between XPRS and WOG (Alfadley et al., 2020).

All three instruments caused minimal apical transportation, below the acceptable 0.15 mm (Freire et al., 2011; Wu et al., 2000). This aligns with studies showing minimal apical transportation with XPRS compared with other instruments (Alfadley et al., 2020; Kabil et al., 2021; Shaheen and Elhelbawy, 2022). Factors influencing canal transport include root

canal morphology, instrument design, alloys, and movement (Bürklein and Schäfer, 2013). In this study, coronal pre-flaring was performed for the PTN and WOG groups, according to the product recommendations, but not for the XPRS group. This flaring has the potential to reduce canal curvature, improve instrument control, and reduce apical transportation (Patel and Rhodes, 2007).

The centering ratio assesses an instrument's ability to remain central to a shaped canal. In the mandibular and maxillary molars, XPS was as central as PTN (X2) or WOG (primary) (Bayram et al., 2022; Kabil et al., 2021). This study found that all rotary groups had similar centering abilities, even with larger PTN (X3) and WOG (medium). PTN and WOG had significantly better centering at the middle and apical levels than at the coronal level. The flexibility and guiding tip of the NiTi alloy may aid in precise negotiation while maintaining the center (Kandaswamy et al., 2009; Ruddle, 2016; Song et al., 2004). Coronal pre-flaring may also have helped PTN and WOG maintain centers in the middle and apical areas (Elnaghy and Elsaka, 2014). Variations in dentin removal, RDT, canal transportation, and centering ability across studies are expected due to differences in samples, instrument sizes, and methodologies. In addition, an earlier XPS version was used instead of the more recent XPRS.

Two broken instruments were discovered in the XPRS group during third root canal preparation. Cyclic fatigue and torsional fractures are the typical causes of instrument breakage (Bürklein and Schäfer, 2013). XPRS has higher cyclic fatigue resistance to failure but lower torque (Silva et al., 2018). A previous study discovered that XPRS fractured after being used six times with severe canal curvature (60.0°) and mild radius (10.0 mm) (Alfadley et al., 2020). This study, which repeatedly used XPRS in severely and more abruptly curved canals, may have contributed to breakage after the third use (Parashos et al., 2004). Curved areas reduce instruments' torsional resistance (Jamleh et al., 2021), suggesting caution with the multiple uses in such canals. Starting root canal preparation with a single instrument with an ISO diameter of 15 and progressing to a diameter of 30 may also increase the resistance to the instrument because of the limited canal width (Webber et al., 2020). Further investigation of these aspects is necessary.

CBCT was used to assess dentin thickness in this study as it prevents specimen degradation and dentin loss during sectioning, making it valuable for clinical research (Mangal et al., 2018). Additionally, a strong correlation between CBCT and micro-CT for dentin thickness has been reported (Xu et al., 2017). CBCT with a 0.30-mm voxel size is clinically acceptable, despite its slight tendency to overestimate compared with direct measurement (Bunn et al., 2020). However, this study used a 0.08-mm voxel for better resolution (Brüllmann and Schulze, 2015). Additionally, thinner CBCT slices improved the assessment accuracy compared to previous studies (Akhlaghi et al., 2015; Pauwels et al., 2015; Sousa et al., 2022).

Although root canal curvature varies, this study used CBCT and ImageJ software to evaluate and control the curvature angle and radius to comparable degrees. Furthermore, the Concentric Circle Plug-in for ImageJ is a novel tool that provides precise measurements of dentin thickness (Rasband, 2007). This approach eliminates examiner

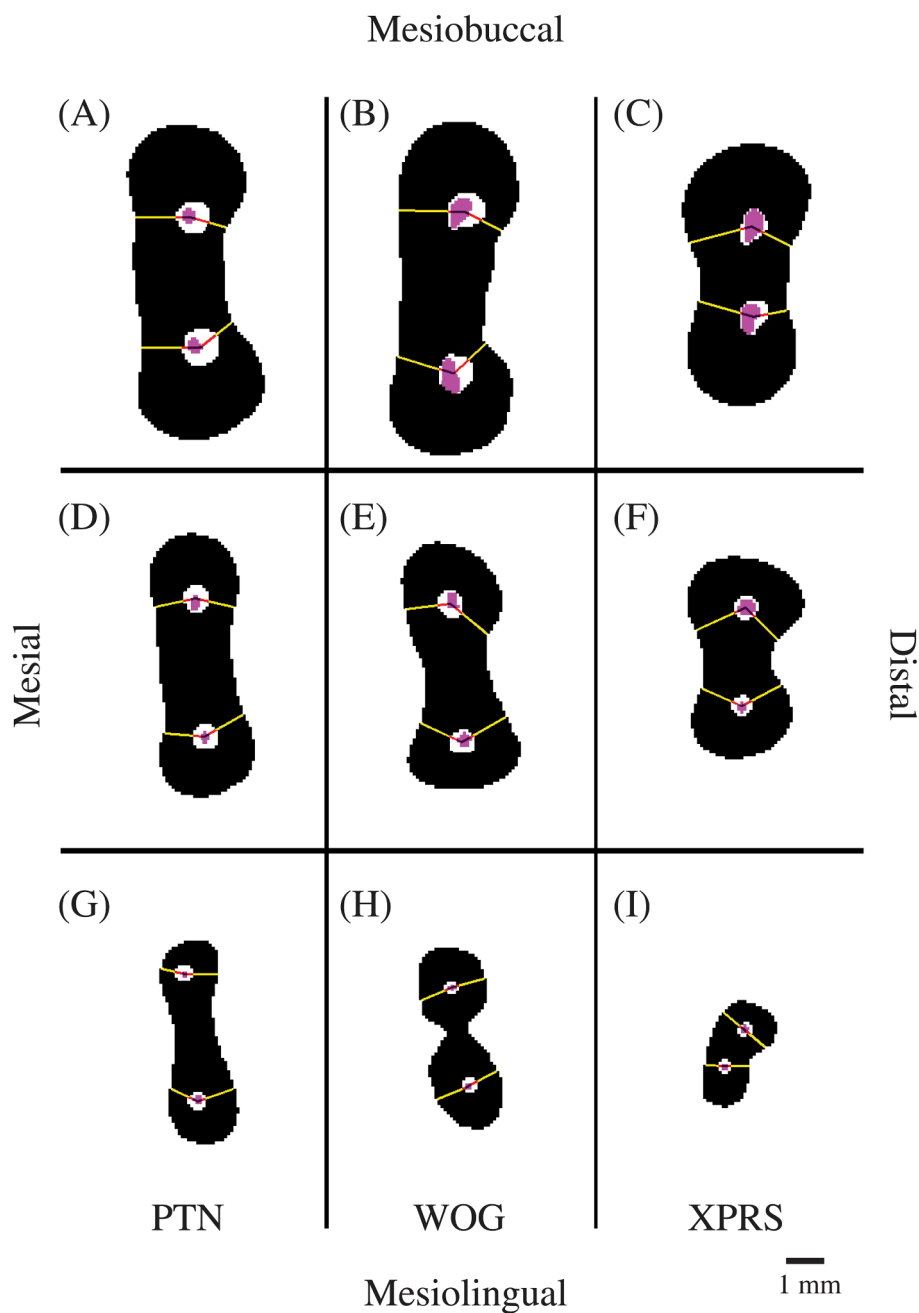


Fig. 2. Cross-sectional images of two superimposed mesial root canals aligned pre- and post-instrumentation show canal changes at the coronal (A–C), middle (D–F), and apical (G–I) levels in ProTaper Next, WaveOne Gold, and XP-endo Rise Shaper groups, together with dentin removal (red line) and remaining dentin thickness (yellow line) in each canal measured using ImageJ software. Purple and white areas indicate pre-instrumentation canal and dentin removal areas, respectively.

Table 4
Median (mm) of canal transportation and centering ratio in three root canal levels.

Level	Transportation			Centering ratio		
	PTN	WOG	XPRS	PTN	WOG	XPRS
Coronal	-0.258 ^{A,*}	-0.229 ^{A,*}	-0.116 ^{A,#}	0.353 ^{A,*}	0.390 ^{A,*}	0.425 ^{A,*}
Middle	0.008 ^{B,*,#}	0.019 ^{B,*}	-0.044 ^{A,#}	0.767 ^{B,*}	0.652 ^{B,*}	0.627 ^{A,*}
Apical	0.033 ^{B,*}	0.010 ^{B,*}	0.038 ^{B,*}	0.700 ^{B,*}	0.508 ^{B,*}	0.505 ^{A,*}

Negative values indicate distal transportation, while positive values indicate mesial transportation. Different superscript majuscules and symbols in the transportation or centering ratio indicate significant differences between levels and rotary systems, according to Kruskal-Wallis and Mann-Whitney U tests ($p < 0.05$).

Abbreviations: PTN, ProTaper Next; WOG, WaveOne Gold; XPRS, XP-endo Rise Shaper.

calibration and simplifies canal change measurements before and after instrumentation at the same location.

These three factors may jeopardize the reproducibility of this type of study. Although the mesiodistal curvature was identified, the buccolingual curvature may also affect canal transportation (Cunningham and Senia, 1992; Leseberg and Montgomery, 1991). Variations in root canal diameter due to periodontitis and unknown age may lead to an asymmetrical distribution of canal transportation and centering ratios. However, canals that could not be negotiated with a #10 K-file were eliminated; these analyzed samples are likely to represent teeth undergoing routine treatment. Additionally, limited slice analysis per root may provide less comprehensive data than micro-CT investigations. Future studies should include samples with multi-directional curvatures, comparable initial canal diameters, and more slices per root.

5. Conclusions

Within the limitations of this study, all rotary instruments exhibited a tendency to remove dentin from the DZ, but to different degrees. In the DZ, XPRS demonstrated better results in terms of coronal transportation and dentin thickness. Regardless of the design, metallurgy, and operating motion, all rotary instruments exhibited comparable centering abilities and minimal apical transportation.

CRedit authorship contribution statement

Chanapa Damkoengsunthorn: Conceptualization, Methodology, Formal analysis, Investigation, Writing – original draft. **Adjabhak Wongviriya:** Methodology, Data curation, Writing – review & editing. **Weeraya Tantanapornkul:** Methodology, Validation. **Kessiri Wisithphrom:** Methodology, Validation. **Kittipong Ketpan:** Methodology. **Thosapol Piyapattamin:** Validation, Writing – review & editing. **Peraya Puapichartdumrong:** Conceptualization, Validation, Visualization, Writing – review & editing, Supervision.

Declaration of Competing Interest

The authors declare that they have no known competing financial interests or personal relationships that could have appeared to influence the work reported in this paper.

Acknowledgments

The authors would like to express their gratitude to Professor Dr. Helmut Glünder for his valuable advice. This research was partially supported by the Faculty of Dentistry at Naresuan University, Thailand.

References

- Abou-Rass, M., Frank, A.L., Glick, D.H., 1980. The anticurvature filing method to prepare the curved root canal. *J. Am. Dent. Assoc.* 101 (5), 792–794.
- Aditya, V., Vandana, K.L., 2023. ImageJ software in periodontics: an insight. *J. Dent. Res. Rev.* 10 (3), 182–184.
- Akhlaghi, N.M., Bajgiran, L.M., Naghdi, A., Behrooz, E., Khalilak, Z., 2015. The minimum residual root thickness after using ProTaper, RaCe and Gates-Glidden drills: a cone beam computerized tomography study. *Eur. J. Dent.* 9 (2), 228–233.
- Alfadley, A., Alrajhi, A., Alissa, H., Alzghaibi, F., Hamadah, L., Alfouzan, K., Jamlah, A., 2020. Shaping ability of XP Endo Shaper file in curved root canal models. *Int. J. Dent.* 2020, 4687045.
- Azim, A.A., Piasecki, L., da Silva Neto, U.X., Cruz, A.T.G., Azim, K.A., 2017. XP shaper, a novel adaptive core rotary instrument: micro-computed tomographic analysis of its shaping abilities. *J. Endod.* 43 (9), 1532–1538.
- Bayram, H.M., Kanber, M., Bayram, E., Ocak, M., Celik, H.H., 2022. Preparation activities of different Ni-Ti file systems in curved canals. *Acta. Sci. Dent. Sci.* 6 (10), 43–51.
- Bergmans, L., Van Cleynbreugel, J., Beullens, M., Wevers, M., Van Meerbeek, B., Lambrechts, P., 2003. Progressive versus constant tapered shaft design using NiTi rotary instruments. *Int. Endod. J.* 36 (4), 288–295.
- Brüllmann, D., Schulze, R.K., 2015. Spatial resolution in CBCT machines for dental/maxillofacial applications-what do we know today? *Dentomaxillofac. Radiol.* 44 (1), 20140204.
- Bunn, D.L., Corrêa, M., Dutra, K.L., Schimdt, T.F., Teixeira, C.D.S., Garcia, L.D.F.R., Bortoluzzi, E.A., 2020. Accuracy of cone-beam computed tomography in measuring the thickness of radicular dentin. *Braz. Dent. J.* 31 (5), 516–522.
- Bürklein, S., Schäfer, E., 2013. Critical evaluation of root canal transportation by instrumentation. *Endod. Topics.* 29 (1), 110–124.
- Cunningham, C.J., Senia, E.S., 1992. A three-dimensional study of canal curvatures in the mesial roots of mandibular molars. *J. Endod.* 18 (6), 294–300.
- de Albuquerque, M.S., Nascimento, A.S., Gialain, I.O., de Lima, E.A., Nery, J.A., de Souza Araujo, P.R., de Menezes, R.F., Kato, A.S., Braz, R., 2019. Canal transportation, centering ability, and dentin removal after instrumentation: a micro-CT evaluation. *J. Contemp. Dent. Pract.* 20 (7), 806–811.
- Elnaghy, A.M., Elsaka, S.E., 2014. Evaluation of root canal transportation, centering ratio, and remaining dentin thickness associated with ProTaper Next instruments with and without glide path. *J. Endod.* 40 (12), 2053–2056.
- Freire, L.G., Gavini, G., Branco-Barletta, F., Sanches-Cunha, R., dos Santos, M., 2011. Microscopic computerized tomographic evaluation of root canal transportation prepared with twisted or ground nickel-titanium rotary instruments. *Oral Surg. Oral Med. Oral Pathol. Oral Radiol. Endod.* 112 (6), e143–e148.
- Gambill, J.M., Alder, M., del Rio, C.E., 1996. Comparison of nickel-titanium and stainless steel hand-file instrumentation using computed tomography. *J. Endod.* 22 (7), 369–375.
- Jamlah, A., Almedlej, R., Alomar, R., Almayouf, N., Alfadley, A., Alfouzan, K., 2021. Evidence for reduced torsional resistance of rotary files under curved position. *Saudi Dent. J.* 33 (7), 614–619.
- Kabil, E., Katić, M., Anić, I., Bago, I., 2021. Micro-computed evaluation of canal transportation and centering ability of 5 rotary and reciprocating systems with different metallurgical properties and surface treatments in curved root canals. *J. Endod.* 47 (3), 477–484.
- Kandaswamy, D., Venkateshbabu, N., Porkodi, I., Pradeep, G., 2009. Canal-centering ability: an endodontic challenge. *J. Conserv. Dent.* 12 (1), 3–9.
- Landini, G., 2004. Align RGB planes v1.7. https://imagej.net/Align_RGB_planes.
- Leseberg, D.A., Montgomery, S., 1991. The effects of Canal Master, Flex-R, and K-Flex instrumentation on root canal configuration. *J. Endod.* 17 (2), 59–65.
- Liang, Y., Yue, L., 2022. Evolution and development: engine-driven endodontic rotary nickel-titanium instruments. *Int. J. Oral Sci.* 14 (1), 12.
- Lim, S.S., Stock, C.J.R., 1987. The risk of perforation in the curved canal: anticurvature filing compared with the stepback technique. *Int. Endod. J.* 20 (1), 33–39.
- Mangal, S., Mathew, S., Murthy, B.V.S., Nagaraja, S., Dinesh, K., Ramesh, P., 2018. Cone-beam computed tomographic evaluation of remaining dentin thickness in bifurcated roots of maxillary first premolars after rotary instrumentation and post space preparation: an in vitro study. *J. Conserv. Dent.* 21 (1), 63–67.
- Nanbunta, P., Puapichartdumrong, P., Tantanapornkul, W., Wisithphrom, K., Piyapattamin, T., 2024. Microscopic evaluation of the mesial root canal diameter, wall thickness, and root concavity in human permanent mandibular first molars. *J. Int. Dent. Med. Res.* 17 (1), 85–92.
- Parashos, P.I., Gordon, I., Messer, H.H., 2004. Factors influencing defects of rotary nickel-titanium endodontic instruments after clinical use. *J. Endod.* 30 (10), 722–725.
- Patel, S., Rhodes, J., 2007. A practical guide to endodontic access cavity preparation in molar teeth. *Br. Dent. J.* 203 (3), 133–144.
- Pauwels, R., Araki, K., Siewerdsen, J.H., Thongvigitmanee, S.S., 2015. Technical aspects of dental CBCT: state of the art. *Dentomaxillofac. Radiol.* 44 (1), 20140224.
- Peters, O.A., Peters, C.I., 2011. Cleaning and shaping the root canal system. In: Hargreaves, K.M., Cohen, S. (Eds.), *Cohen's Pathways of the Pulp*, tenth ed. Mosby Elsevier, St. Louis, pp. 283–348.
- Pruett, J.P., Clement, D.J., Carnes Jr., D.L., 1997. Cyclic fatigue testing of nickel-titanium endodontic instruments. *J. Endod.* 23 (2), 77–85.
- Rasband, W.S., 2007. Concentric Circles. U.S. National Institutes of Health. <http://imagej.net/ij/plugins/concentric-circles.html>.
- Ruddle, C.J., 2016. Single-file shaping technique: achieving a gold medal result. *Dent. Today* 35 (1), 98102–100103.
- Ruddle, C.J., Machtou, P., West, J.D., 2013. The shaping movement: fifth-generation technology. *Dent. Today* 32 (4), 96–99, 94.
- Schneider, S.W., 1971. A comparison of canal preparations in straight and curved root canals. *Oral Surg. Oral Med. Oral Pathol. Oral Radiol.* 32 (2), 271–275.
- Shaheen, N.A., Elhelbawy, N.G.E., 2022. Shaping ability and buckling resistance of TruNatomy, WaveOne gold, and XP-Endo Shaper single-file systems. *Contemp. Clin. Dent.* 13 (3), 261–266.
- Silva, E.J.N.L., Vieira, V.T.L., Belladonna, F.G., Zuolo, A.S., Antunes, H.D.S., Cavalcante, D.M., Elias, C.N., De-Deus, G., 2018. Cyclic and torsional fatigue resistance of XP-endo Shaper and TRUShape instruments. *J. Endod.* 44 (1), 168–172.
- Song, Y.L., Bian, Z., Fan, B., Fan, M.W., Gutmann, J.L., Peng, B., 2004. A comparison of instrument-centering ability within the root canal for three contemporary instrumentation techniques. *Int. Endod. J.* 37 (4), 265–271.
- Sousa, V.C., Alencar, A.H.G., Bueno, M.R., Decurcio, D.A., Estrela, C.R.A., Estrela, C., 2022. Evaluation in the danger zone of mandibular molars after root canal preparation using novel CBCT software. *Braz. Oral Res.* 36, e038.
- Uygun, A.D., Kol, E., Topcu, M.K.C., Seckin, F., Ersoy, I., Tanriver, M., 2016. Variations in cyclic fatigue resistance among ProTaper Gold, ProTaper Next and ProTaper Universal instruments at different levels. *Int. Endod. J.* 49 (5), 494–499.
- Vertucci, F.J., 1984. Root canal anatomy of the human permanent teeth. *Oral Surg. Oral Med. Oral Pathol.* 58 (5), 589–599.
- Webber, M., Piasecki, L., Jussiani, E.I., Andreello, A.C., Dos Reis, P.J., Azim, K.A., Azim, A., 2020. Higher speed and no glide path: a new protocol to increase the efficiency of XP shaper in curved canals—an in vitro study. *J. Endod.* 46 (1), 103–109.
- Wu, M.K., Fan, B., Wesselink, P.R., 2000. Leakage along apical root fillings in curved root canals. Part I: effects of apical transportation on seal of root. *J. Endod.* 26 (4), 210–216.
- Xu, J., He, J., Yang, Q., Huang, D., Zhou, X., Peters, O.A., Gao, Y., 2017. Accuracy of cone-beam computed tomography in measuring dentin thickness and its potential of predicting the remaining dentin thickness after removing fractured instruments. *J. Endod.* 43 (9), 1522–1527.
- Yang, Q., Cheung, G.S., Shen, Y., Huang, D., Zhou, X., Gao, Y., 2015. The remaining dentin thickness investigation of the attempt to remove broken instrument from mesiobuccal canals of maxillary first molars with virtual simulation technique. *BMC Oral Health* 15, 87.
- Zhou, G., Leng, D., Li, M., Zhou, Y., Zhang, C., Sun, C., Wu, D., 2020. Root dentine thickness of danger zone in mesial roots of mandibular first molars. *BMC Oral Health* 20 (1), 43.
- Zupanc, J., Vahdat-Pajouh, N., Schäfer, E., 2018. New thermomechanically treated NiTi alloys – a review. *Int. Endod. J.* 51 (10), 1088–1103.